Batteries & Supercaps

Research Article
doi.org/10.1002/batt.202400401

Chemistry Europe
European Chemical Societies Publishing

www.batteries-supercaps.org

Development of Tailored Hydrocarbon-Based Pentablock Copolymer Membranes for Sodium-Polysulfide Flow Batteries

Michelle Lehmann,*[a] Tomonori Saito,[a] Mohamed Kamaludeen,[b] and Guang Yang*[a]

Long-duration energy storage (LDES) technologies are pivotal for the adoption of renewables like wind and solar. Non-aqueous redox flow batteries (NARFBs) with a sodium-polysulfide hybrid system feature high energy density independent of power density, yet face challenges with polysulfide shuttling. This study investigates a hydrocarbon-based penta-block copolymer membrane, Nexar, to mitigate crossover effects by balancing TFSI conversion and their crosslink density. The membranes are annealed to induce crosslinking for reducing electrolyte uptake and enhancing mechanical stability while demonstrating excellent ionic conductivity. The hydrocarbon-based membranes address environmental concerns associated with perfluoroalkyl substances and improve the performance and durability of NARFBs. Our findings suggest that annealed Nexar membranes with tailored TFSI functionality offer a scalable, cost-effective solution for enhancing the efficiency of high-capacity energy storage systems, pivotal for grid integration of renewable sources.

Introduction

Long-duration energy storage (LDES) technologies are essential for enabling the widespread adoption of renewable energy sources such as wind and solar on the electric grid and are projected to grow by 800% over the next 30 years in the U.S.[1] Redox flow batteries (RFBs) have emerged as an ideal solution for LDES applications due to their unique capability to decouple energy density from power density.[2,3] However, most technologies today use vanadium or other platinum group metals, which are proven to be very expensive and cost prohibitive to scale. Additionally, current LDES technologies are struggling to meet the DOE targets set forth in the Long-Duration Storage Shot,[4] as the U.S. is currently at a significant disadvantage with respect to the supply chain of critical materials, especially in upstream segments (i.e., raw material acquisition and refining) as well as midstream component production (i.e., cathodes and anodes). This highlights the need to develop technologies that are less reliant on critical materials. Non-aqueous RFBs (NARFBs) offer a promising alternative as they utilize supporting electrolytes with wider operating voltage windows (>3 V) and diverse redox couples.[2,5] Of particular interest is the hybrid NARFB, which combines an alkali metal anode, such as sodium, with a polysulfide catholyte, mirroring secondary Na–S batteries. However, challenges such as polysulfide shuttling are exacerbated in these NARFB systems due to the need to keep the sodium-sulfur complex in the soluble regime (Na_2S_x, x = 5–8),[6] necessitating the development of new membranes that exhibit robust mechanical properties, excellent electrochemical stability, high ionic conductivity, and low polysulfide permeability.

Ceramic membranes, such as Na^+ β″-Al_2O_3, have been widely utilized in polysulfide-based flow batteries due to their ability to eliminate the crossover of catholyte species. However, they are typically only available in thick formats (e.g., 1 mm thick sheets), likely due to their fragile mechanical properties. Porous separators are also commonly used for NARFBs due to being inexpensive and chemically stable, but their large pores result in significant crossover of soluble polysulfide species.[5,7] Polymers that exhibit intrinsic microporosity (PIMs) have attracted attention for use in aqueous flow batteries due to their excellent selectivity.[8–10] Additionally, PIMs have been utilized in Li–S batteries, though they seem to require the addition of a secondary polymer (e.g., polyethylene oxide) to achieve reasonable performance.[11,12]

Previously, we demonstrated that the dense polymeric structure of Nafion significantly slows Na_2S_x crossover compared to a porous separator but found that Nafion adversely reacts with Na metal, forming a resistive passivation layer during extended cycling.[13,14] Additionally, due to environmental concerns over 'forever' chemicals, the use of perfluoroalkyl substances (PFAS), such as Nafion, needs to be replaced with environmentally friendly hydrocarbon-based membranes. However, the development of hydrocarbon-based membranes for NARFBs is limited.

This study pioneers the development of a hydrocarbon-based polymer tailored for use in sodium-polysulfide flow battery applications. Diverging from the heavily researched PFAS-based membranes, Kraton Corp.'s pentablock copolymer membrane, Nexar, represents an emerging class of hydrocarbon membranes that innovatively combine structural robustness with enhanced ionic conductivity with its unique block-copolymer design. By converting the sulfonic acid moieties within Nexar to TFSI anions and integrating them with a glyme-based plasticizer, we pre-

[a] M. Lehmann, T. Saito, G. Yang
Chemical Sciences Division, Oak Ridge National Laboratory, PO Box 2008, MS6124, Oak Ridge, TN 37831, United States
E-mail: lehmannm@ornl.gov
yangg@ornl.gov

[b] M. Kamaludeen
U.S. DOE Office of Electricity, Washington, DC 20585, United States

Supporting information for this article is available on the WWW under https://doi.org/10.1002/batt.202400401

Research Article
doi.org/10.1002/batt.202400401
Chemistry Europe
European Chemical Societies Publishing

viously demonstrated a remarkable increase in ionic conductivity by four orders of magnitude.[15] However, while the TFSI-modified Nexar membranes display enhanced ionic conductivity, they encounter challenges with considerable swelling that adversely affects their mechanical integrity. To address this issue, we fabricated blends of the sulfonic acid and TFSI forms of the polymer and applied thermal annealing to induce physical crosslinking. This study provides a thorough examination of how annealed blends of modified and unmodified Nexar influence the structural and electrochemical properties of the membranes and, by extension, the overall performance of sodium-polysulfide batteries. This study lays the groundwork for further optimization the Nexar-based membranes and advance the application of hydrocarbon membranes in non-aqueous energy storage technologies.

Experimental

Synthesis and Fabrication of Membranes. Nexar™ pentablock terpolymer, poly(*t*-butylstyrene-*b*-hydrogenated isoprene-*b*-sulfonated styrene-*b*-hydrogenated isoprene-*b*-*t*-butylstyrene), poly(tBS − HI − sS − HI − tBS), (MD-9200) was kindly provided by Kraton Corporation. The polymer is synthesized by anionic polymerization followed by hydrogenation of the poly(isoprene) block and selective sulfonation of styrene to obtain an ion exchange capacity (IEC) of 2.0 meq/g. The molecular weight of each block in unsulfonated form (tBS − HI − S − HI − tBS) is approximately 15 − 10 − 28 − 10 − 15 kg/mol.[16–18] The Nexar TFSI polymer was synthesized using a procedure we reported previously and has an IEC of 1.6 meq/g.[15] The appropriate weight ratios of the sulfonic acid and TFSI forms of the polymer (in proton form) were dissolved in 1:1 (w/w) toluene/1-propanol to form a 13 wt% polymer solution. The membranes were fabricated by tape casting onto silicon coated mylar, air drying overnight, then annealing at 120 °C for 30 min. The membranes were exchanged to sodium form by soaking in a 1 M NaOH aqueous solution for 24 h. The solution was replaced with fresh NaOH three times, then rinsed well with deionized water. After air-drying for 24 h, the membranes were cut to size and dried at 85 °C under vacuum before being transferred to an argon filled glovebox. The membranes were approximately 50 μm thick. The weight percent of TFSI polymer utilized is denoted by the number following the TFSI label, i.e., TFSI90 contains 90 wt% TFSI and 10 wt% sulfonated polymers.

Membrane Characterizations. The glass transition temperature (T_g) of the membranes was determined by dynamic mechanical analysis (DMA) using a TA Instruments Q800 DMA. Samples of a 15×5 mm size were measured at an operating frequency of 1 Hz and heated at a rate of 10 °C/min from −80 to 250 °C. T_g of the membranes was recorded from the loss modulus peaks.

The electrolyte uptake of the membranes soaked in a 1 M $NaPF_6$/diglyme electrolyte solution was determined using:

$$?Uptake\ (\%) = \frac{m_w - m_d}{m} \times 100$$

where m_w is the mass of the polymer after soaking in the electrolyte solution for at least 48 hours and m_d is the mass of the dry polymer. The swelling ratio of the membranes was obtained using:

$$Swelling\ ratio\ (\%) = \frac{l_w - l_d}{l_d}$$

where l_w is the length of the polymer after soaking in the electrolyte solution for at least 48 hours and l_d is the length of the dry polymer.

Electrochemical Characterizations. Samples for electrochemical measurements were prepared in a glovebox and equilibrated in the electrolyte solution for at least 48 h. Tests were performed using a Biologic VMP3 potentiostat and EC-Lab® software. Samples were sealed in a CR2032 coin cell and sandwiched between 12 mm Na foil. The impedance was measured while heating from 20–60 °C for 2 cycles. The frequency range of 1 MHz–1 Hz was used, with a 6 mV AC signal. Sodium stripping/plating tests were performed at room temperature at ±100 μA/cm² for 0.5 h in each half cycle. Critical current density measurements were performed at current densities from ±50–800 μA/cm² for 0.5 h in each half cycle. Open circuit voltage and full cell cycling measurements were performed using CR2032 cells containing a 0.95 cm diameter carbon paper (Sigracet 36AA, Fuel Cell Store) containing 11 μL of catholyte and a 12 mm sodium metal anode. The membrane (equilibrated in 1 M $NaPF_6$/diglyme) was blotted to remove excess electrolyte and then assembled in a cell containing catholyte-soaked carbon paper and sodium metal. Open circuit voltage measurements used a 0.25 M Na_2S_8 in 0.5 M $NaPF_6$/diglyme catholyte. Full cell cycling measurements utilized a 0.25 M Na_2S_8 in 1 M $NaPF_6$ 0.2 M $NaNO_3$/5:1 tetraglyme:diglyme (v/v) catholyte and 20 μL of 1 M $NaPF_6$ 0.2 M $NaNO_3$/5:1 tetraglyme:diglyme (v/v) as an anolyte. The cells with the TFSI membranes utilized a Celgard 3501 interlayer between the Na metal and membrane to improve mechanical stability.

Results and Discussion

Nexar is a hydrocarbon pentablock terpolymer that forms mechanically robust membranes and microphase-separated ionic domains. We initially made annealed membranes utilizing the sulfonated form of the polymer, as the styrene sulfonate functional group can form covalent as well as physical crosslinks.[19–21] The annealed sulfonated membranes exhibited insignificant electrolyte uptake and negligible ionic conductivity. Thus, we wanted to utilize the sulfonated membranes with the TFSI form of the polymer as a method to reduce electrolyte uptake of the TFSI membranes (Figure 1). Membranes were fabricated by dissolving appropriate weight ratios of the sulfonic acid and TFSI forms of Nexar in toluene/1-propanol and tape casting. The dry membranes were then annealed at 120 °C for 30 min to achieve the crosslinking reaction and then converted from proton to sodium form. The IEC of the membranes increases with the increase in sulfonic acid polymer content in the blend, from 1.58–1.76 meq/g for the TFSI 100 and TFSI 60, respectively.

Successful crosslinking of the membranes was determined by DMA. The membranes were tested in proton form due to the sodium form of the membranes having strong ionic interactions, which increases the T_g of the ionic block to temperatures close to the decomposition temperature of the polymers (>450 °C),[15,22] which would obscure the influence of crosslinking. The unannealed TFSI and sulfonic acid forms of the membranes exhibit a softening point at 115 °C and 90 °C, respectively, corresponding to the T_g of polystyrene TFSI and polystyrene sulfonic acid[15,23,24] (Figure 2a). Upon annealing, both samples exhibit an extended plateau above their respective T_g's and no crossover point between E′ and E″, indicating either covalent or physical cross-

Research Article
doi.org/10.1002/batt.202400401
Chemistry Europe
European Chemical Societies Publishing

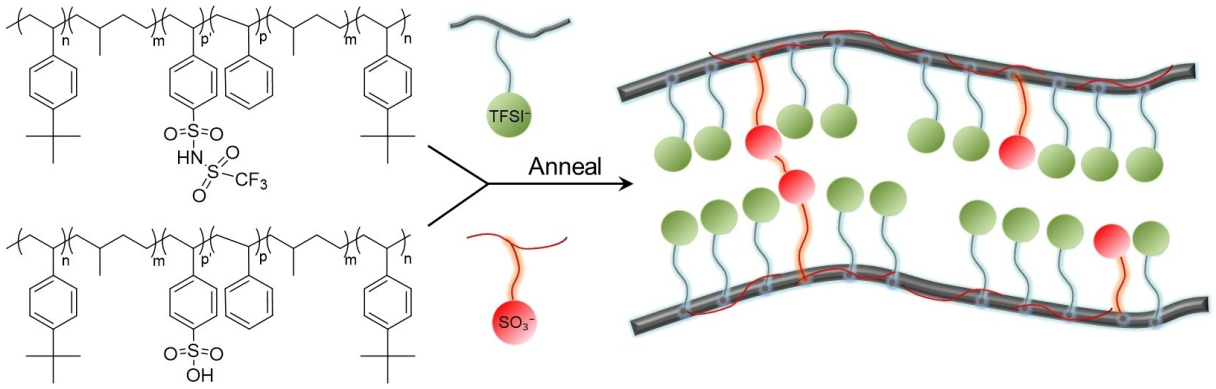

Figure 1. Schematic of TFSI and sulfonated forms of Nexar, and cartoon of possible crosslinking sites.

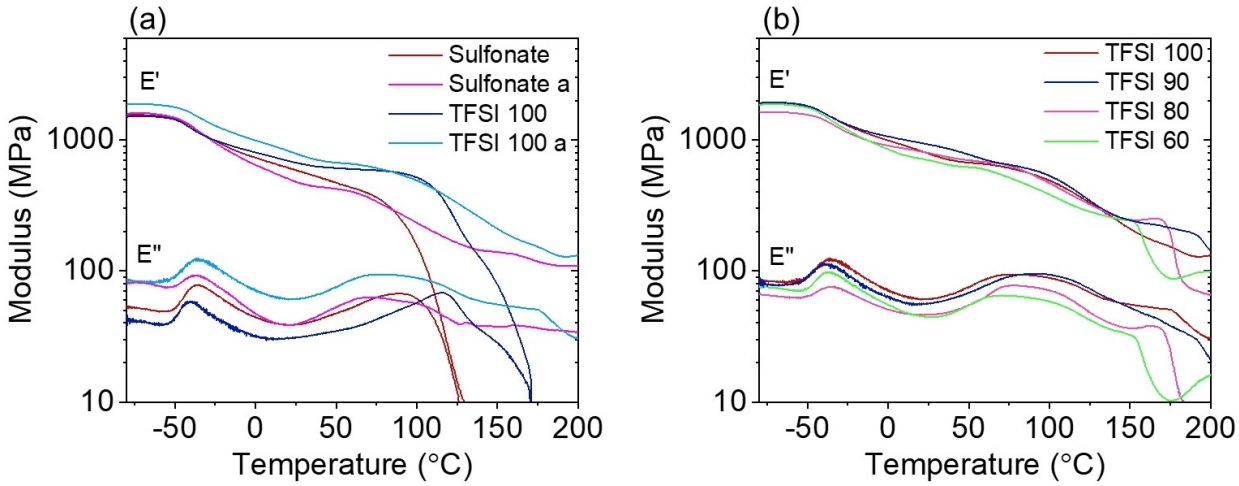

Figure 2. Dynamic mechanical analysis of the membranes. (a) Unannealed and annealed (denoted with 'a') sulfonic acid and H^+ TFSI membranes, and (b) annealed blends of sulfonic acid and H^+ TFSI membranes.

linking occurred to enable the membranes to stay in a solid amorphous state. As seen in Figure 2b, the TFSI/sulfonic acid blends have a similar E′ and E″ profile as the annealed TFSI sample. The TFSI 60 sample exhibits a broader transition between 60 and 120 °C, similar to the annealed sulfonic acid membrane, due to the higher sulfonate content within this membrane.

The electrolyte uptake of the membranes is an important parameter as it influences membrane mechanical properties, conductivity, and redox species permeability. As seen in Figure 3a, electrolyte uptake decreases with an increase in sulfonate polymer content. The TFSI 100 membrane has the highest electrolyte uptake of 124%, but lower than the unannealed version, which had an electrolyte uptake of 156% in a similar solvent/salt system.[15] The lower uptake for the annealed sample supports the DMA result that crosslinking occurs during annealing for the TFSI 100 sample, likely due to ionic crosslinking. With the addition of a small portion of sulfonated polymer, electrolyte uptake decreases to 80% for TFSI 90, while further addition of sulfonated polymer has a limited influence on electrolyte uptake. The swelling ratio of the membranes (linear dimensional change) does not change significantly from TFSI 100 (16.1%) to TFSI 90 (15.4%). Meanwhile, the thickness change of the membranes decreases from 35% to 22%, respectively. Even with the reduction in electrolyte uptake, the mechanical properties of the membranes are not quite adequate for flow battery applications and will likely need a support layer, a practice commonly utilized for non-aqueous flow-battery membranes.[5,25–27]

The addition of sulfonated polymer to the TFSI form has a significant impact on the ionic conductivity of the membranes (Figure 3). The conductivity decreases from 0.25 mS/cm to 5.4×10^{-3} mS/cm for the TFSI 100 and TFSI 60 membranes, respectively. The reduction in ionic conductivity with increasing sulfonated polymer content contrasts with the increase in membrane IEC and indicates that the annealed sulfonated polymer actually inhibits ionic conductivity in a non-aqueous electrolyte. Thus, the TFSI 100 and TFSI 90 samples were selected for further evaluation.

To determine the maximum operating current density of the membranes, critical current density measurements were conducted at room temperature in sodium symmetric cells (Figure 4a). The cells were cycled at current densities of 50–800 μA/cm^2. The TFSI membranes exhibit stable cycling at 50–200 μA/cm^2 and exhibit spikes in the overpotential at 500 μA/cm^2. Nafion 212 also exhibits unstable cycling upon reaching 500 μA/cm^2 current

Research Article
doi.org/10.1002/batt.202400401
Chemistry Europe
European Chemical Societies Publishing

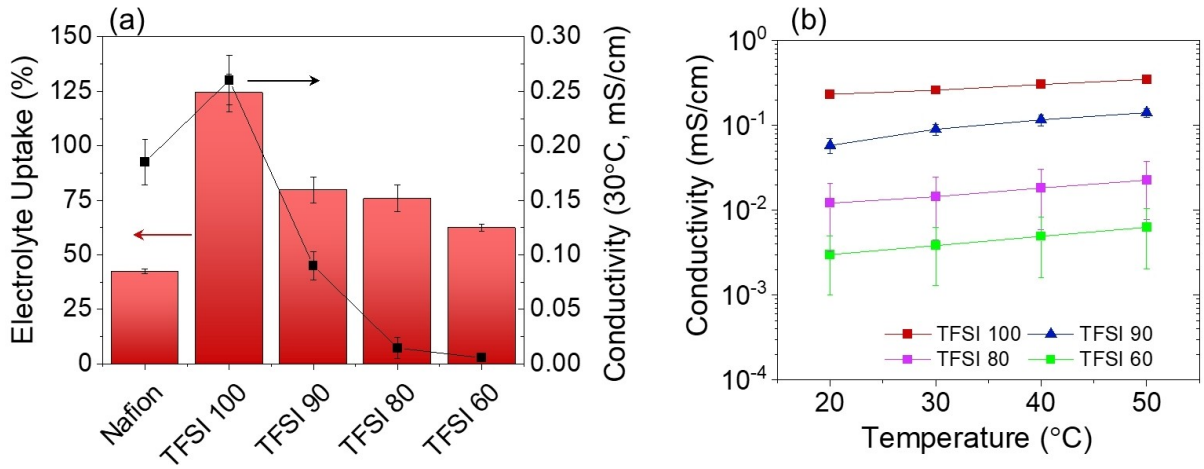

Figure 3. (a) Ionic conductivity (30 °C) and electrolyte uptake, and (b) ionic conductivity as a function of temperature of membranes equilibrated in 1 M $NaPF_6$/diglyme.

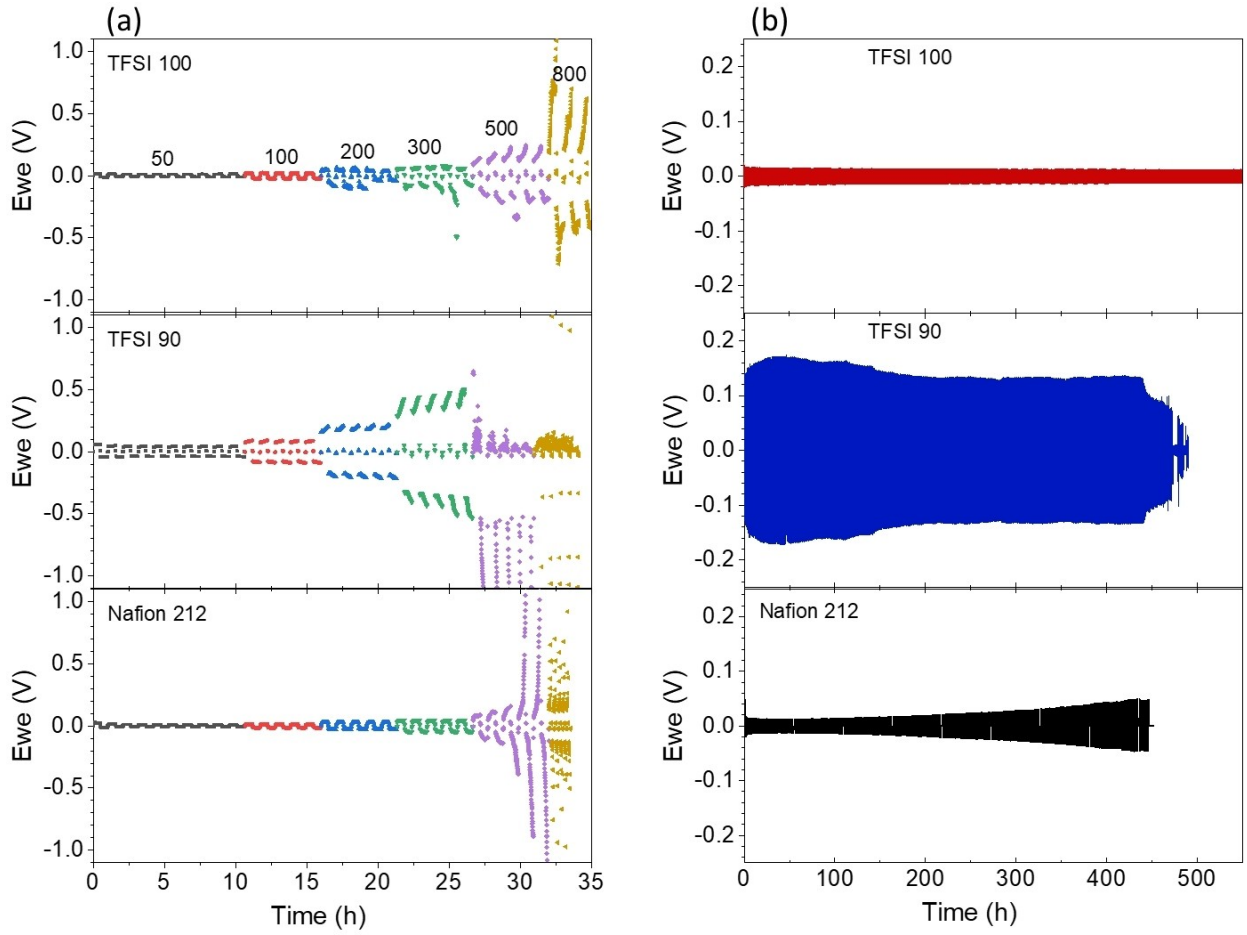

Figure 4. (a) Overpotential of membranes at various current densities. (b) Sodium symmetric cell stripping/plating measurements for the various membranes, using 1 M $NaPF_6$/diglyme electrolyte at a current density of 100 μA/cm^2.

density. Extended stripping/plating evaluation was performed at 100 μA/cm^2. One notable difference in the cycling profile of Nafion compared to the TFSI membranes is the increase in overpotential over time for Nafion. The increase is due to the instability of Nafion against the sodium metal, causing a resistive solid-electrolyte interface layer to be formed,[13,28] and suggests that the non-perfluorinated hydrocarbon membranes are more electrochemically stable against sodium metal.

Crossover of polysulfide species, Na_2S_x through the membrane can be monitored by a self-discharge process in which Na_2S_8

Research Article
doi.org/10.1002/batt.202400401

crosses through the membrane and is reduced at the anode to form insoluble products. Na_2S, which is insoluble in diglyme, is the expected thermodynamic endpoint for such reactions. In a full cell assembly, the open circuit voltage, E_{we}, decays over time for all three membranes, though the TFSI membranes exhibit improved blocking of polysulfide crossover compared to Nafion 212 (Figure 5). Although Nafion has low electrolyte uptake in comparison to the TFSI membranes, it has the highest crossover with an OCV of 1.95 V at 10 h. The crossover rate polysulfides through Nafion can be improved by utilizing a thicker membrane,[13,14] but this comes at the expense of increased membrane resistance. In general, redox species crossover follows a tradeoff where high conductivity (or uptake) equates to high crossover. This trend holds when comparing the TFSI membranes, but not when they are compared to Nafion, indicating a different mode of crossover through the membranes exists between the TFSI membranes and Nafion. It is difficult to quantify what modes of crossover occur for each membrane, as crossover can occur by diffusion through the ionic domains, the backbone region, or a combination of both. A recent study by McCormack et al. suggests that in non-aqueous systems, the primary mode of redox species crossover may be through the non-ionic backbone regions of the polymer,[29,30] though this is likely highly dependent on the system utilized.

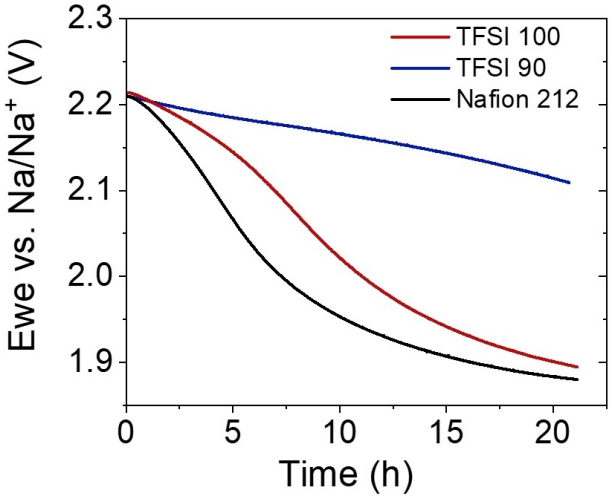

Figure 5. Open circuit voltage evolution of the Na | membrane | Na_2S_x full cells.

We further evaluate the full cell performance of the TFSI membranes in a coin cell configuration. A Celgard interlayer was added between the Na metal and membrane to enhance the mechanical stability of the membranes during cell assembly. The galvanostatic cycling profiles of the Na-Na_2S_x cells at various cycles are shown in Figure 6a. Nafion has the largest initial capacity compared to its TFSI counterparts (due to a different polysulfide utilization mechanism, which is discussed below), but the capacity quickly fades to a level below that of the TFSI membranes. As seen in Figure 6b, the capacity retention of the TFSI membranes significantly outperforms that of Nafion. More specifically, the capacity retention of TFSI 100 is 62% and TFSI 90 is 75%, which is in sharp contrast to that of Nafion at merely 18%. The sharp capacity fade for Nafion is partially due to its instability against sodium metal, as demonstrated in Figure 4b, and a different polysulfide transition mechanism. The initial performance of Nafion is similar to that previously reported by Bauer et al. for a Nafion coated porous polypropylene separator, where an initial capacity of 400 mAh/g_s was achieved with a capacity retention of 87% after 20 cycles utilizing a solid sulfur cathode.[7] Although a direct comparison with literature is difficult due to limited studies on the membrane for Na–S flow battery applications. It is important to note that while these tests employed a static coin cell setup, the materials used, such as carbon paper, were selected for their compatibility and potential seamless transition into flow battery systems. Secondary Na–S battery studies often utilize a solid sulfur cathode or a binder-free carbon nanofiber interlayer to improve capacity retention, which are not suitable for a flow battery application.[31–33]

The galvanostatic cycling of the full cells depicted as differential capacity plots demonstrate the influence of membrane composition on the polysulfide transition kinetics (Figure 7). To study a full transition cycle of the sodium polysulfide, we focus on

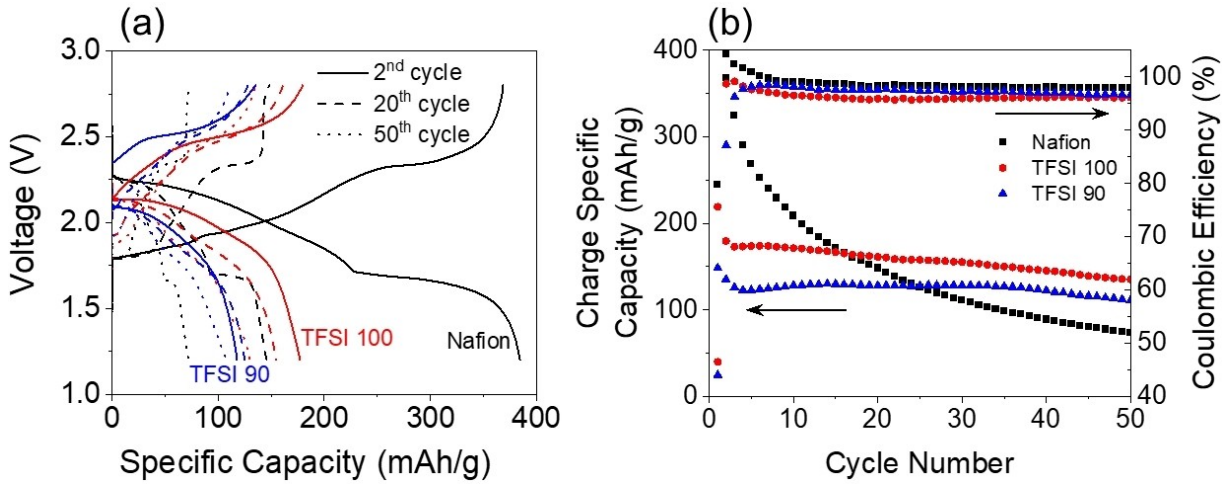

Figure 6. (a) Galvanostatic cycling profiles of Na-Na_2S_x cells using different membranes and (b) the corresponding specific charge capacity (normalized a sulfur loading of 0.7 mg) of the samples over 50 cycles. Cells were cycled at 0.2 C (330 mA/cm^2) at room temperature.

Research Article
doi.org/10.1002/batt.202400401
Chemistry Europe
European Chemical Societies Publishing

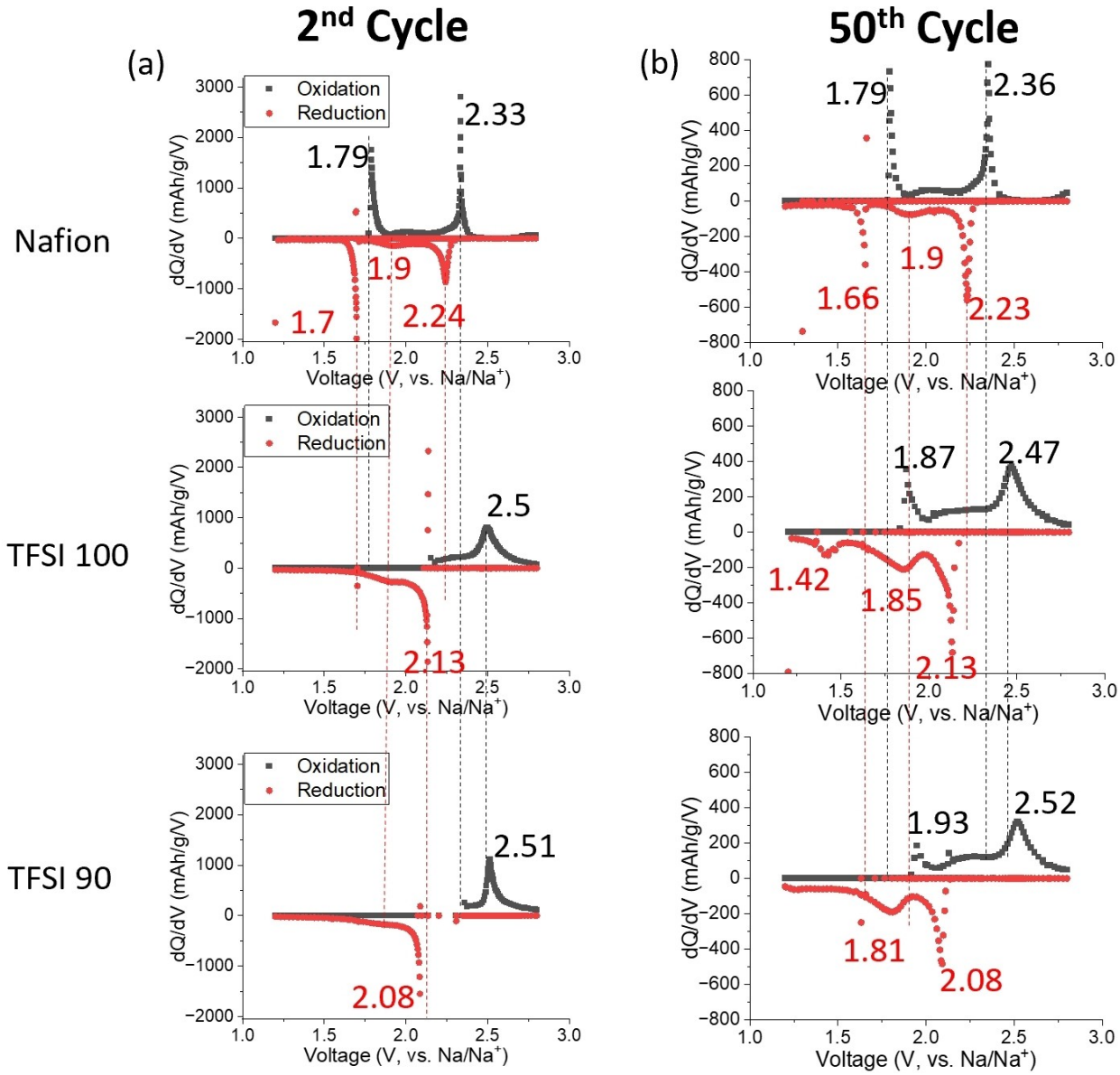

Figure 7. Differential capacity profile of different Na | membrane | Na_2S_x full cells at (a) 2nd cycle and (b) 50th cycle.

the 2nd cycle of each sample, as our starting catholyte is Na_2S_8 which has an open circuit voltage (2.21 V) intermediate in the cycling window. Typically, reduction peaks close to 1.65 V and 2.2 V represent a liquid-solid and solid-liquid transition, respectively.[34] In the 2nd cycle, Nafion exhibits the highest reduction peak at 2.24 V, representing a lower energy barrier for the solid S to liquid Na_2S_8 transition. Another point to note is that the Na-Na_2S_x cell with Nafion exhibits a sharp reduction peak at 1.7 V, corresponding to the transition from sparingly soluble Na_2S_4 to insoluble Na_2S_x ($x < 4$). Such a peak is absent for the TFSI 100 and TFSI 90 membranes. Clearly, the liquid-solid transition is lacking for the TFSI 100 and TFSI 90 samples. In the 50th cycle, additional reduction peaks become more distinguished for TFSI 100 and TFSI 90 at 1.85 V and 1.81 V, respectively, corresponding to the transition between Na_2S_8 and Na_2S_5. Overall, compared with Nafion, the polysulfide catholyte with the TFSI 100 and TFSI 90 membranes mainly involves the liquid-liquid transition regime. This fact explains their lower initial capacity but improved capacity retention due to reduced sedimentation involving the formation of insoluble polysulfide species (Na_2S_x where $x < 4$).

Conclusions

A hydrocarbon-based pentablock copolymer membrane, Nexar, was tailored by blending the TFSI and sulfonated forms of the polymer, and subsequent crosslinking by annealing. The electrolyte uptake and conductivity of the annealed membranes decreased with increasing sulfonic acid content, and the membrane with just 10 wt% of the sulfonic acid form of the polymer (90 wt% TFSI of the form) exhibited an electrolyte uptake of 78% compared with 125% for the TFSI 100 sample. These modified

Nexar membranes demonstrated improved electrochemical stability against sodium metal and lower polysulfide crossover compared to Nafion. Additionally, the TFSI-based membranes show improved capacity retention (62–75%) in a Na-Na_2S_x battery compared to Nafion, which exhibited a fast capacity fade to 18% after 50 cycles. Overall, the tailored Nexar-based membranes demonstrate promise as a hydrocarbon-based alternative to Nafion and a path toward obtaining high-performance membranes for redox flow batteries containing an alkali metal anode to support DOE Long Duration Storage Shot objectives.

Author Contributions

ML performed experiments and wrote most of the manuscript. MK wrote a section of the manuscript. GY and TS provided overall guidance for experiments and manuscript preparation. GY performed management of research planning and execution.

This manuscript has been authored by UT-Battelle, LLC under Contract No. DE-AC05-00OR22725 with the U.S. Department of Energy. The United States Government retains and the publisher, by accepting the article for publication, acknowledges that the United States Government retains a non-exclusive, paid-up, irrevocable, world-wide license to publish or reproduce the published form of this manuscript, or allow others to do so, for United States Government purposes. The Department of Energy will provide public access to these results of federally sponsored research in accordance with the DOE Public Access Plan (http://energy.gov/downloads/doe-public-access-plan).

Acknowledgements

This work is supported by the U.S. Department of Energy, Office of Electricity (OE), Energy Storage Division. We would like to thank Kraton Corporation for providing Nexar samples and for fruitful discussions.

Conflict of Interests

The authors declare no conflict of interest.

Data Availability Statement

The data that support the findings of this study are available from the corresponding author upon reasonable request.

Keywords: Hydrocarbon membranes · Redox flow batteries · Sodium sulfur batteries

[1] *Energy Information Administration, U. S. Department of Energy, U. S. Battery Storage Market Trends* https://www.eia.gov/analysis/studies/electricity/batterystorage/pdf/battery storage.pdf**2018**, Last accessed Sept. 14 2020.
[2] K. Gong, Q. Fang, S. Gu, S. F. Y. Li, Y. Yan, *Energy Environ. Sci.* **2015**, *8* (12), 3515–3530.
[3] S.-H. Shin, S.-H. Yun, S.-H. Moon, *RSC Adv.* **2013**, *3*(24), 9095–9116.
[4] Long Duration Storage Shot. **2021**. https://www.energy.gov/eere/long-duration-storage-shot (accessed 05/27/2024).
[5] M. L. Lehmann, L. Tyler, E. C. Self, G. Yang, J. Nanda, T. Saito, *Chem* **2022**, *8* (6), 1611–1636.
[6] E. C. Self, J. L. Tyler, J. Nanda, *J. Electrochem. Soc.* **2021**, *168* (8), 080540.
[7] I. Bauer, M. Kohl, H. Althues, S. Kaskel, *Chem. Commun.* **2014**, *50* (24), 3208–3210.
[8] R. Tan, A. Wang, R. Malpass-Evans, R. Williams, E. W. Zhao, T. Liu, C. Ye, X. Zhou, B. P. Darwich, Z. Fan, *Nat. Mater.* **2020**, *19* (2), 195–202.
[9] R. Tan, A. Wang, C. Ye, J. Li, D. Liu, B. P. Darwich, L. Petit, Z. Fan, T. Wong, A. Alvarez-Fernandez, *Adv. Sci. (Weinh)* **2023**, *10* (20), 2206888.
[10] I. S. Chae, T. Luo, G. H. Moon, W. Ogieglo, Y. S. Kang, M. Wessling, *Adv. Energy Mater.* **2016**, *6* (16), 1600517.
[11] C. Li, A. L. Ward, S. E. Doris, T. A. Pascal, D. Prendergast, B. A. Helms, *Nano Lett.* **2015**, *15* (9), 5724–5729.
[12] Y. Ji, K. Yang, M. Liu, S. Chen, X. Liu, B. Yang, Z. Wang, W. Huang, Z. Song, S. Xue, *Adv. Funct. Mater.* **2021**, *31* (47), 2104830.
[13] M. L. Lehmann, E. C. Self, T. Saito, G. Yang, *Membranes (Basel)* **2023**, *13* (8), 700.
[14] J. L. Tyler, R. L. Sacci, M. L. Lehmann, G. Yang, T. A. Zawodzinski, J. Nanda, *J. Phys. Chem. C* **2022**, *126*, 21188–21195.
[15] M. L. Lehmann, G. Yang, J. Nanda, T. Saito, *Macromolecules* **2022**, *55* (17), 7740–7751.
[16] J. H. Choi, C. L. Willis, K. I. Winey, *J. Membr. Sci.* **2012**, *394*, 169–174.
[17] Y. Fan, C. J. Cornelius, *J. Mater. Sci.* **2013**, *48* (3), 1153–1161.
[18] G. Geise, B. Freeman, D. Paul, *Polymer* **2010**, *51* (24), 5815–5822.
[19] N. W. DeLuca, Y. A. Elabd, *J. Membr. Sci.* **2006**, *282* (1–2), 217–224.
[20] P. Knauth, L. Pasquini, B. Maranesi, K. Pelzer, R. Polini, M. Di Vona, *Fuel Cells* **2013**, *13* (1), 79–85.
[21] J.-W. Lee, J. H. Lee, M. Kim, S. M. Hong, C. M. Koo, *J. Nanosci. Nanotechnol.* **2013**, *13* (5), 3606–3610.
[22] P. Balding, R. Borrelli, R. Volkovinsky, P. S. Russo, *Macromolecules* **2022**, *55* (5), 1747–1762.
[23] C. Jangu, A. M. Savage, Z. Zhang, A. R. Schultz, L. A. Madsen, F. L. Beyer, T. E. Long, *Macromolecules* **2015**, *48* (13), 4520–4528.
[24] T. Saito, H. D. Moore, M. A. Hickner, *Macromolecules* **2010**, *43* (2), 599–601.
[25] J.-H. Kim, S. Ryu, S. Maurya, J.-Y. Lee, K.-W. Sung, J.-S. Lee, S.-H. Moon, *RSC Adv.* **2020**, *10* (9), 5010–5025.
[26] E. Cho, J. Won, *J. Power Sources* **2016**, *335*, 12–19.
[27] J. Jung, J. Won, S. S. Hwang, *J. Membr. Sci.* **2020**, *595*, 117520–117530.
[28] X. B. Cheng, R. Zhang, C. Z. Zhao, Q. Zhang, *Chem. Rev.* **2017**, *117* (15), 10403–10473.
[29] P. M. McCormack, G. M. Koenig Jr., G. M. Geise, *ACS Appl. Mater. Interfaces* **2021**, *13* (41), 49331–49339.
[30] P. M. McCormack, H. Luo, G. M. Geise, G. M. Koenig Jr., *J. Power Sources* **2020**, *460*, 228107–228117.
[31] X. Yu, A. Manthiram, *J. Phys. Chem. C* **2014**, *118* (40), 22952–22959.
[32] X. Yu, A. Manthiram, *Chem. Mater.* **2016**, *28* (3), 896–905.
[33] D. Zhou, Y. Chen, B. Li, H. Fan, F. Cheng, D. Shanmukaraj, T. Rojo, M. Armand, G. Wang, *Angew. Chem. Int. Ed.* **2018**, *57* (32), 10168–10172.
[34] X. Yu, A. Manthiram, *ChemElectroChem* **2014**, *1* (8), 1275–1280.

Manuscript received: June 20, 2024
Revised manuscript received: September 13, 2024
Accepted manuscript online: October 10, 2024
Version of record online: November 12, 2024